

1 **SUPPORTING INFORMATION**

2 **Identifying and quantifying the intermediate processes during nitrate dependent iron(II)**
3 **oxidation**

4 *James Jamieson^{1,2}, Henning Prommer^{1,2,3 *}, Anna H. Kaksonen^{3,4}, Jing Sun^{1,3}, Adam Siade^{1,2,3}, Anna
5 Yusov⁵ and Benjamin Bostick⁶*

6 ¹*University of Western Australia, School of Earth Sciences, Western Australia, 6009, Australia*

7 ²*National Centre for Groundwater Research and Training, Australia*

8 ³*CSIRO Land and Water, Private Bag No. 5, Wembley, Western Australia, 6913, Australia*

9 ⁴*School of Pathology and Laboratory Medicine, University of Western Australia, 35 Stirling Highway,
10 Crawley, Western Australia 6009, Australia*

11 ⁵*Department of Chemistry, Barnard College, 3009 Broadway, New York, NY 10027, United States*

12 ⁶*Lamont-Doherty Earth Observatory, PO Box 1000, 61 Route 9W, Palisades, NY 10964, United States*

13

14

15

16

17 Pages: 10 (including the cover page)

18

19

Figures: 4

20

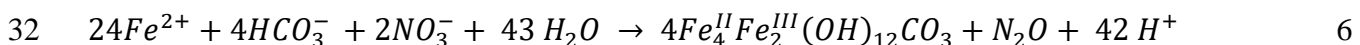
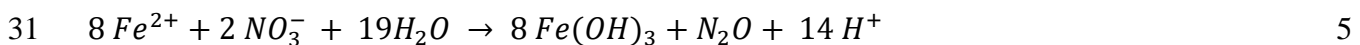
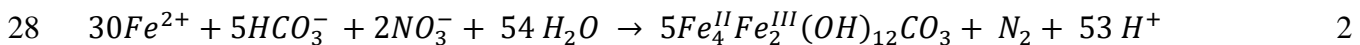
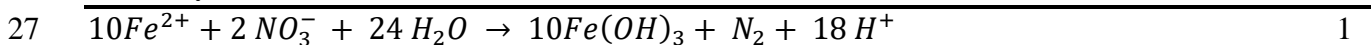
Tables: 4

21

22

23

24 **Table S1:** Thermodynamic Gibbs free energies for potential enzymatic NDFO where nitrate
 25 reduction is coupled to Fe oxidation. Bolded reactions are those used in this study for calculating the
 26 thermodynamic kinetic term F_T .



33 ${}^1\Delta G^{o'} = -100.4 \frac{kJ}{mol}, {}^2\Delta G^{o'} = -50.47 \frac{kJ}{mol}, {}^3\Delta G^{o'} = -69.9 \frac{kJ}{mol}, {}^4\Delta G^{o'} = -40$

34 $53 \text{ kJ/mol}, {}^5\Delta G^{o'} = -85.8 \text{ kJ/mol}, {}^6\Delta G^{o'} = -45.8 \text{ kJ/mol}$

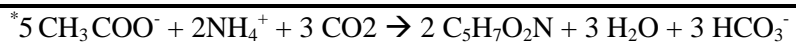
35

36

37

38 **Table S2:** Theoretical substrate conversion and growth stoichiometry for *Acidovorax* sp. strain
 39 BoFeN1 and *Paracoccus denitrificans* strain Pd 1222 from literature data sets used in this study for
 40 development of biogeochemical model. Chemodenitrification is ignored giving a conservative
 41 estimate of the electrons available for nitrate reduction. Molar concentration of biomass growth are
 42 calculated values taken from models that assume a biomass yield coefficient of 13.92 g per mol of
 43 acetate, a representative cell formula of C₅H₇O₂N and a cell mass of 0.1 pg/cell.

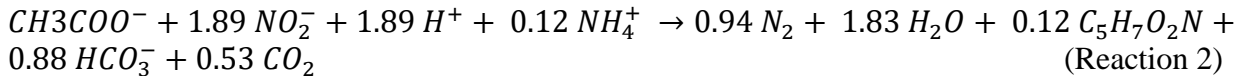
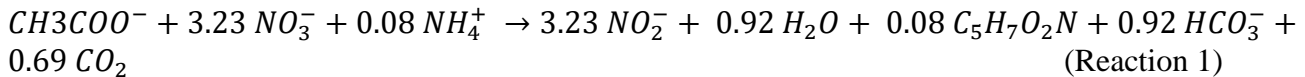
Electron Balance (Supplied/Consumed)	Experiments with varying acetate for BoFeN1				<i>Paracoccus denitrificans</i>
	Acetate(mM)	0	2	5	
Electrons Supplied					
Cell Mass [#] (mM)		2.7E-04	6.4E-04	6.2E-04	3.63E-04
Acetate assimilated (mM) [*]		0.67	1.60	1.54	0.91
Acetate Oxidized (mM)		1.33	3.40	3.46	4.09
Acetate (electrons)		10.63	27.22	27.70	32.74
FeSO ₄ (electrons)		2.00	8.00	6.50	6.50
Total Electrons Supplied		12.6	35.2	34.2	39.2
Electrons Consumed					
Nitrate Consumed (mM)		5	10	10	10
Nitrite formed (mM)		1	0.9	3.5	1.13
Nitrate - N ₂ (electrons)		20	45.5	32.5	44.35
Nitrate-Nitrite (electrons)		2	1.8	7	2.26
Total Electrons Consumed		22	47	40	47
Electrons Recovered (%)		174	134	116	119



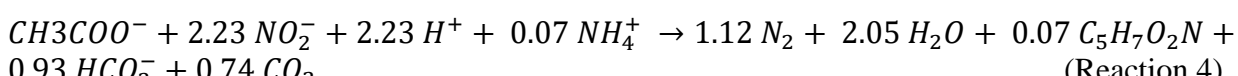
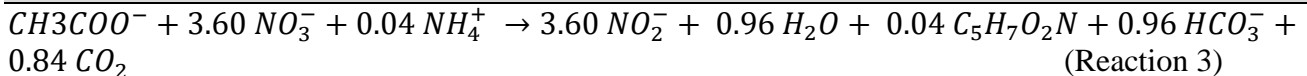
[#]Taken from model input where not stipulated in original source material.

45 **Table S3:** Overall stoichiometric reactions for denitrification for all bacteria species investigated in
 46 simulation S1a. Full stoichiometric reactions were derived using the principles and protocol from
 47 Rittmann and McCarty (2001).

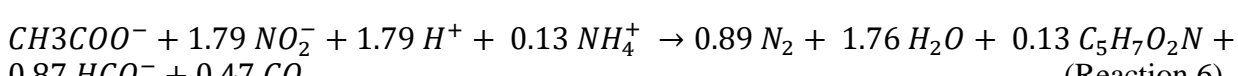
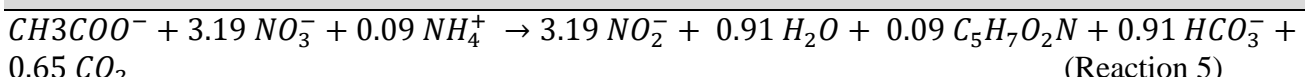
48 *Acidovorax* spp. strain BoFeN



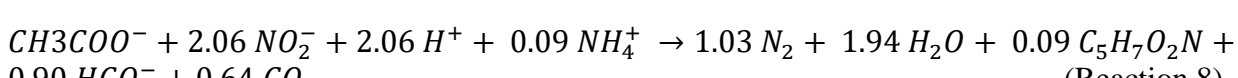
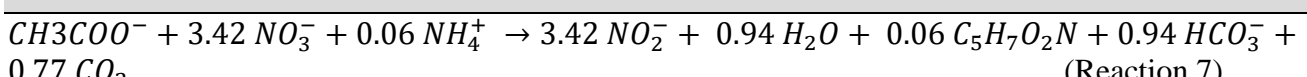
53 *Acidovorax* spp. strain TSPY



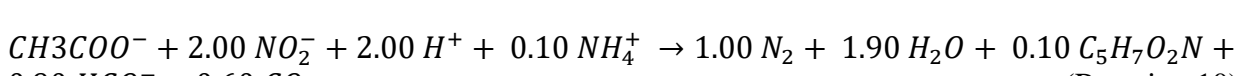
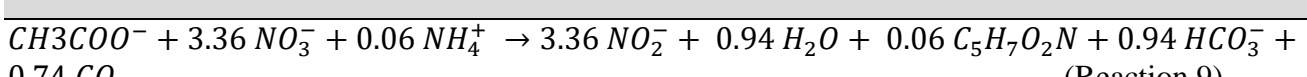
58 *Acidovorax* spp. strain 2AN



63 *Paracoccus denitrificans* strain Pd 1222



68 *Pseudogulbenkiania* strain 2002



73 (Biomass is represented as $C_5H_7O_2N$)

74

75

76

77

78

79

80

81 **Table S4:** All model parameters estimated by PEST/PSO for model variant S1a simulations

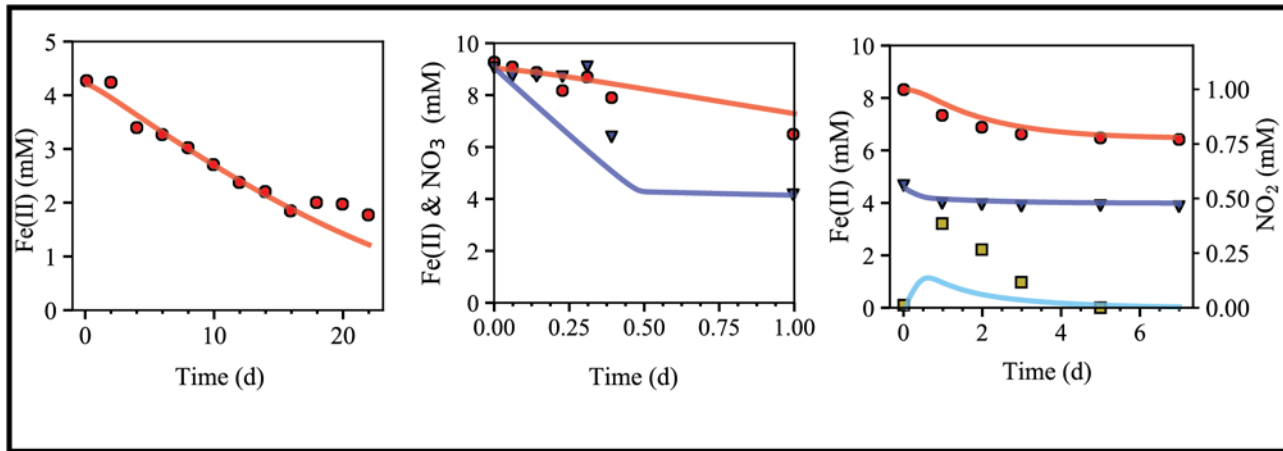
Parameter name	Lower limit	Upper limit	Estimated value	Posterior variance	Posterior standard deviation	Estimated value minus two standard deviations*	Estimated value plus two standard deviations*
Efficiency parameter (ϵ) for calculation of full stoichiometric reactions							
ϵ_1 (BoFeN1)	1.50E-01	5.00E-01	3.02E-01	1.76E-04	1.33E-02	2.8E-01	3.3E-01
ϵ_2 (TPSY)	1.50E-01	5.00E-01	2.07E-01	3.42E-04	1.85E-02	1.7E-01	2.4E-01
ϵ_3 (2AN)	1.50E-01	5.00E-01	3.01E-01	2.16E-04	1.47E-02	2.7E-01	3.3E-01
ϵ_4 (Pd 1222)	1.50E-01	5.00E-01	2.60E-01	2.21E-04	1.49E-02	2.3E-01	2.9E-01
ϵ_5 (2002)	1.50E-01	5.00E-01	2.75E-01	2.37E-04	1.54E-02	2.4E-01	3.1E-01
Parameters for microbial respiration of nitrate reduction to nitrite							
K_D	1.00E-07	1.00E-02	2.18E-03	6.52E-01	8.08E-01	1.0E-07	1.0E-02
K_A	1.00E-07	1.00E-03	2.38E-05	2.08E-02	1.44E-01	1.0E-07	1.0E-03
k_1	1.00E-06	1.00E-03	7.99E-05	9.999E-01	9.999E-01	1.0E-06	1.0E-03
Parameters for microbial respiration of nitrite reduction to dinitrogen							
K_D	1.00E-07	1.00E-03	2.25E-05	8.34E-01	9.13E-01	1.0E-07	1.0E-03
K_A	1.00E-07	1.00E-03	3.50E-06	8.11E-04	2.85E-02	1.0E-07	1.0E-03
k_1	1.00E-06	1.00E-03	1.10E-04	4.58E-04	2.14E-02	1.0E-06	1.0E-03
Encrustation							
Inhibition	1.00E-04	1.00E-02	7.59E-03	7.28E-01	8.53E-01	1.0E-04	1.0E-02

*If the interval goes beyond specified upper or lower limits, the limit value is listed instead.

82

83

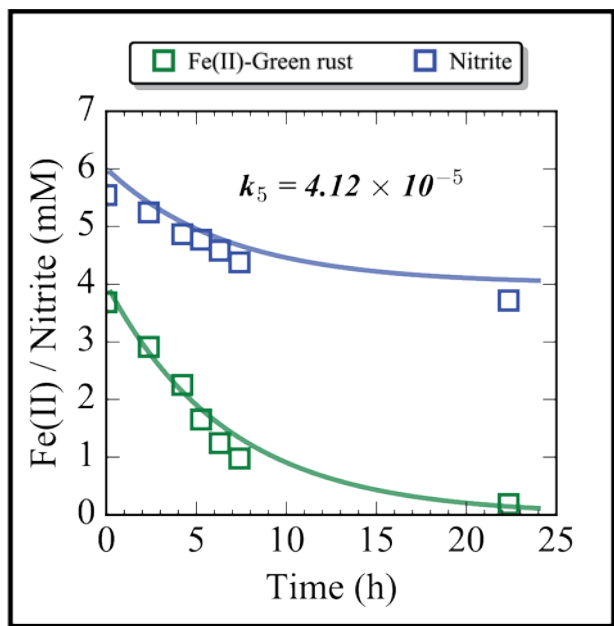
84 **Figure S1:** Enzymatic Fe(II) oxidation rate for all strains investigated were calibrated from batch
 85 experiments with solution media containing nitrate but where Fe(II) was added as the sole electron
 86 donor. Selected data from these ‘chemolithoautotrophic’ batch experiments were used as biogenic
 87 nitrite from heterotrophic nitrate reduction could be ignored. Results are presented for *Acidovorax*
 88 spp. strains BoFeN1 (left), TSPY (middle) and 2AN (right) from Klueglein and Kappler¹, Carlson et
 89 al.² and Chakraborty et al.³, respectively. Solid lines represent simulation results while symbols
 90 represent observed concentrations for total Fe(II) (red circle), nitrate (blue down triangle) and nitrite
 91 (yellow square).



92
 93
 94

95 **Figure S2:** Green rust Fe(II) oxidation rate. Rate constant (k_5) calibrated from data collected by
96 Hansen et al⁴.

97



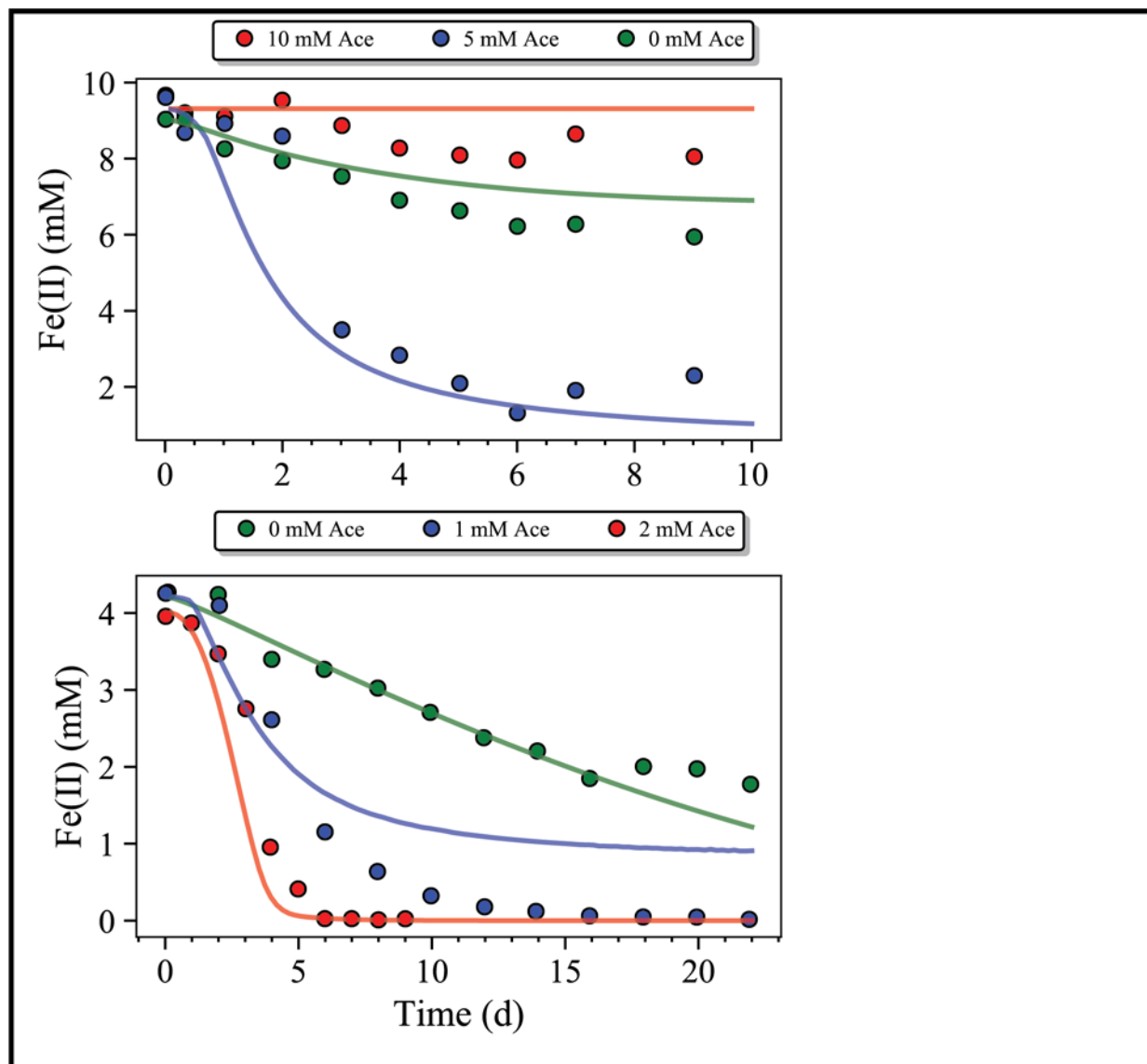
98

99

100

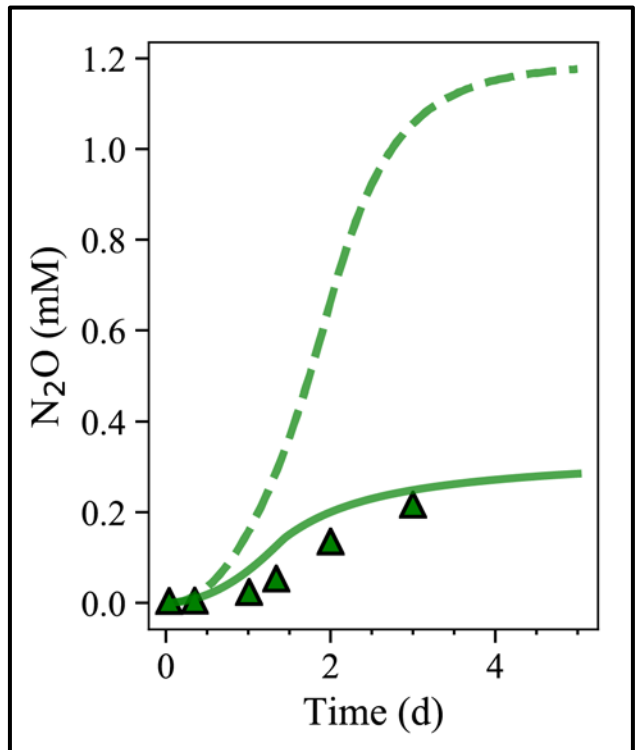
101
102
103
104

Figure S3: Simulation of Fe(II) concentrations (solid lines) during NDO in *Acidovorax* sp. strain BoFeN1 (bottom panel) and TPSY (top panel) growth incubations at different acetate (Ace) concentrations. Symbols represent observed concentrations of Fe(II) from experiments within Kappler et al.⁵ and Carlson et al.²



105

106 **Figure S4:** S1a (solid line) and S2 (dashed line) model simulation results for nitrous oxide for strain
107 *Acidovorax sp.* strain TPSY. Symbols represent observed concentrations of nitrous oxide from
108 experiments within Carlson et al.²



109

110 **REFERENCES**

- 111 (1) Klueglein, N.; Kappler, A. Abiotic oxidation of Fe(II) by reactive nitrogen species in
112 cultures of the nitrate-reducing Fe(II) oxidizer *Acidovorax* sp. BoFeN1 – questioning the existence
113 of enzymatic Fe(II) oxidation. *Geobiology* **2013**, *11*, 180-190.
- 114 (2) Carlson, H. K.; Clark, I. C.; Blazewicz, S. J.; Iavarone, A. T.; Coates, J. D. Fe(II)
115 Oxidation Is an Innate Capability of Nitrate-Reducing Bacteria That Involves Abiotic and Biotic
116 Reactions. *Journal of Bacteriology* **2013**, *195*, 3260-3268.
- 117 (3) Chakraborty, A.; Roden, E. E.; Schieber, J.; Picardal, F. Enhanced Growth of
118 *Acidovorax* sp. Strain 2AN during Nitrate-Dependent Fe(II) Oxidation in Batch and Continuous-
119 Flow Systems. *Applied and Environmental Microbiology* **2011**, *77*, 8548-8556.
- 120 (4) Hansen, H. C. B.; Borggaard, O. K.; Sørensen, J. Evaluation of the free energy of
121 formation of Fe(II)-Fe(III) hydroxide-sulphate (green rust) and its reduction of nitrite. *Geochimica et*
122 *Cosmochimica Acta* **1994**, *58*, 2599-2608.
- 123 (5) Kappler, A.; Schink, B.; Newman, D. K. Fe(III) mineral formation and cell
124 encrustation by the nitrate-dependent Fe(II)-oxidizer strain BoFeN1. *Geobiology* **2005**, *3*, 235-245.

125